

RSC Advances



This is an *Accepted Manuscript*, which has been through the Royal Society of Chemistry peer review process and has been accepted for publication.

Accepted Manuscripts are published online shortly after acceptance, before technical editing, formatting and proof reading. Using this free service, authors can make their results available to the community, in citable form, before we publish the edited article. This *Accepted Manuscript* will be replaced by the edited, formatted and paginated article as soon as this is available.

You can find more information about *Accepted Manuscripts* in the [Information for Authors](#).

Please note that technical editing may introduce minor changes to the text and/or graphics, which may alter content. The journal's standard [Terms & Conditions](#) and the [Ethical guidelines](#) still apply. In no event shall the Royal Society of Chemistry be held responsible for any errors or omissions in this *Accepted Manuscript* or any consequences arising from the use of any information it contains.

Free Standing Silica Thin Films with Highly Ordered Perpendicular Nanopores

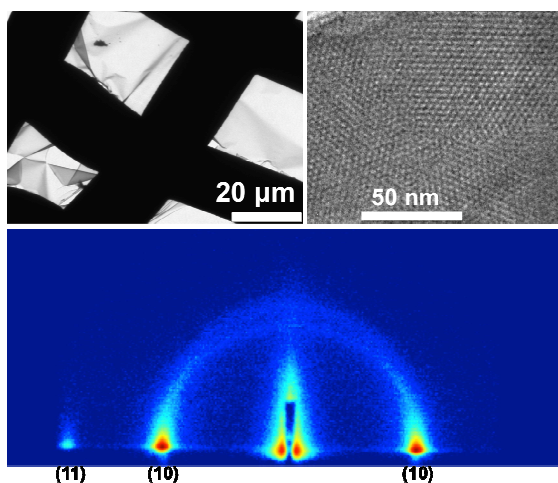
*Jifang Cheng^a, Somilkumar J. Rathi^b, Paul Stradins^c, Gitti L. Frey^d, Reuben T. Collins^e and S. Kim Ratanathanawongs Williams^{*a}*

^aDepartment of Chemistry and Geochemistry, Colorado School of Mines, Golden, CO, 80401, USA; ^bThe School for Engineering of Matter, Transport and Energy, Arizona State University, Tempe, AZ, 85287, USA; ^cNational Renewable Energy Laboratory, 1617 Cole Blvd, Golden, CO, 80401, USA; ^dDepartment of Materials Engineering, Technion-Israel Institute of Technology, Haifa 32000, Israel; ^eDepartment of Physics, Colorado School of Mines, Golden, CO, 80401, USA

krwillia@mines.edu, Fax: +1-303-273-3629, Tel: +1-303-273-3245

RECEIVED DATE

Table of contents entry



Free standing silica thin films with perpendicular ordered nanopores were obtained by electro-assisted self-assembly and subsequent detachment from PEDOT:PSS coated indium tin oxide (ITO) substrates.

The novelty of this work lies in the use of a conductive polymer layer to facilitate the synthesis and preparation of free standing mesoporous silica thin films.

Abstract

The synthesis of mesoporous silica thin films on nontraditional conductive substrates using an electro-assisted self-assembly (EASA) technique is described. This work extends prior demonstrations of EASA by exploring the effects of precursor sol pH, temperature, and substrate roughness and describes a new approach to synthesizing a mesoporous silica film that is detachable from the substrate. The latter uses a conductive polymer as a planarization layer for successful EASA on indium-tin oxide coated glass (ITO) and as a sacrificial layer that can be subsequently dispersed in water to release the silica film. This is a particularly important development because it opens up possibilities for synthesizing perpendicularly aligned nanoporous silica on a broad range of surfaces and non-conductive substrates and producing free standing nanostructured thin films. The silica films that are produced have well ordered hexagonally packed mesopores that are vertical to the substrate surface. The thicknesses of these mesoporous silica films were examined by scanning electron microscopy (SEM) and determined to be controllably variable between ~100 – 200 nm. Transmission electron microscopy (TEM) showed organized porous structural features that were approximately 3 nm in diameter. Grazing-incidence small angle X-ray scattering (GISAXS) analysis yielded an ~4.2 nm pore-to-pore distance and confirmed that a $p6mm$ orientation persisted throughout the 6 cm² mesoporous silica film samples.

1. Introduction

Mesoporous silica materials have drawn a great deal of attention because of their process-tunable pore diameters that can be varied from 2 to 30 nm, large surface areas and pore volumes¹⁻⁵, and stability in air and liquids. These advantages make them ideal

hosts or “hard templates” for the preparation of ordered nanostructure arrays of metals⁶, metal oxides^{7,8}, semiconductor materials⁹⁻¹¹, and carbon-based nanostructures⁶, with applications in catalysis, electrochemistry, semiconductor devices, and photovoltaics. Moreover, the fabrication of films with well defined nanopores oriented perpendicular to the substrate surface allows direct through-film access and opens up new application areas where, for example, electrical or molecular transport along the length of the pores is important. These include nanowire arrays for electronic devices, solution based selective sensors and preconcentrators.¹² Furthermore, the ability to detach the mesoporous films from the solid substrates will yield high pore density films that can be used as membranes or biosensors.¹³ Synthesizing free-standing through-film nanoporous arrays with well defined size and orientation across large areas is extremely desirable and very challenging.

Mesoporous silica thin films are often prepared by dip-coating, printing, or spin-coating silica-based precursors on to flat substrates¹⁴. Such processes generally lead to randomly oriented pores or limited domain ranges with oriented pores. Evaporation induced self-assembly (EISA)¹³ is a versatile method for preparing films on flat surfaces. However, the mesopores of the EISA films^{13,15} generally form parallel to the substrate surface. Combining EISA with an applied field¹⁶⁻¹⁸ has been demonstrated as a method for achieving perpendicular pore orientation. In 1997, Firouzi¹⁹ and Tolbert²⁰ created an aligned surfactant- silica mesophase on the centimeter scale by applying a high magnetic field during film formation. Yamauchi²¹ further demonstrated the influence of high magnetic fields on the orientation of a block copolymer surfactant that was used to form nanochannels in silica films. Although, these studies demonstrated the possibility of

producing perpendicularly oriented pores, the use of a high magnetic field may not be practical for the synthesis of large area films. Richman²² obtained vertically oriented hexagonally packed nanoporous silica films by nanometer-scale epitaxy. This method required a precise lattice match between the pores of the surfactant-silica film and the cubic mesoporous substrates. Teng²³ developed a Stöber-solution growth approach to obtain mesoporous silica thin films with perpendicular channels. However, the film formation took several days under strictly controlled high temperatures due to the slow film growth speed (2 nm h⁻¹). Other approaches for orienting pores perpendicular to the substrate include optical lithography²⁴, ion track etching²⁴ electrochemical etching²⁵, and anodization²⁴. These methods are usually limited to > 10 nm pores or disordered pore structures.

Recently, Walcarius²⁶ and Goux²⁷ developed an intrinsically simple and fast electro-assisted self-assembly (EASA) method to prepare silica films with pores that are orthogonal to the surface of metals, glassy carbon, and conductive metal oxide substrates. EASA exploits the electrochemically driven self-assembly of cationic surfactant molecules²⁷, the electro-generation of hydroxyl ions²⁶, and silica condensation²⁶ at the cathode surface. The first process leads to ordered surfactant self-assembly and alignment, the second catalyzes sol polycondensation and the third results in silica sol condensation around the surfactant nanostructures. The net result is the formation of a thin silica film consisting of hexagonally packed nanochannels that are aligned perpendicular to the cathode surface. EASA requires a conductive substrate that can serve as the cathode. Mesoporous silica film formation on gold, platinum, copper, indium tin oxide, and glassy carbon substrates has been successfully demonstrated over 10 mm²

areas. Pore sizes are varied between 2.6 and 3.1 nm depending on the carbon chain length of the alkyltrimethylammonium bromide surfactant C_n TAB ($n=14-18$).

Thus far, EASA has been performed only on conductive substrates. In addition, while removal of silica films for electron microscopy was accomplished by mechanically scraping the cathode, this removal process is not a practical method for obtaining large, substrate free, film areas for further study or applications. Furthermore, the adhesion²⁸ of thin silica films to noble metal (such as Au, Pt, etc.,) substrates is weak and leads to defects in the form of cracks. The local detachment from the substrate causes changes in the film morphology during surfactant removal due to the reduction in the surface energy.²⁹ Conductive metal oxides present a surface that could be used with EASA with advantages that include good adhesion to silica thin film and good conductivity. However, the effect of the relatively high surface roughness³⁰ of glass-coated conductive metal oxide substrates on the formation of uniform perpendicular oriented mesoporous films is undetermined. This roughness can be reduced by coating the metal oxide with conductive polymers.³¹

This paper describes the successful synthesis of mesoporous silica films on two non-traditional conductive substrates using the EASA technique and the subsequent detachment of the film from the substrate. Poly(3,4-ethylenedioxythiophene):poly(styrenesulfonate) (PEDOT:PSS) is a conductive polymer that was spin coated onto surfaces such as indium-tin oxide (ITO) to improve the surface flatness and adhesion of silica. This PEDOT:PSS coated ITO will be referred to as P-ITO. The second substrate investigated in this work is a heavily doped n-type silicon wafer, also with a flat surface³² and good attachment to silica²⁸. Synthesis and EASA conditions

are optimized and explanations are given for the successful formation of silica films with mesopores oriented perpendicular to the substrate surface. The process for detaching or lifting off the mesoporous silica film from the P-ITO substrate is also described.

2. Experimental

Synthesis of the mesoporous silica films occurs in different stages starting with preparation of the precursor sol, followed by preparation of the conductive substrates, and ending with electro-assisted self-assembly of rod-shaped surfactant micelles and polycondensation of silica around the micelles at the cathode/substrate surface. Each stage required optimization and was performed as described below. All chemicals were used as purchased without further purification.

2.1. Preparation of precursor sol

A solution was prepared by mixing 0.82g (2.18 mmol) cetyltrimethylammonium bromide (CTAB, 99%, Fluka, Denmark), 20 mL ethanol (95%, Pharmco Products Inc., CT, USA), and 20 mL aqueous 0.1 M NaNO₃ (98%, J.T. Baker Chemical Co., NJ, USA) and adjusting the pH with HCl (37%, Pharmco-AAPER Subsidiaries of Commercial Alcohols Inc., CT, KY, USA). To this solution, 1.52 mL (1.42 g, 6.80 mmol) tetraethyl orthosilicate (TEOS, 98%, Aldrich, MO, USA) was added under stirring. The resulting precursor sol had an optimum [CTAB]:[TEOS] ratio of 0.32 and was allowed to hydrolyze for 2.5 hours^{26,27}. Fresh precursor sol was made for each experiment. The role of the NaNO₃ in the precursor sol was to increase the conductivity of the sol and subsequently facilitate the EASA process. The pH and temperature of the precursor sol were varied to determine optimum conditions for the formation of ordered silica mesopores.

2.2. Preparation of substrates

The conductive substrates used in this work are an indium-tin oxide coated glass (ITO) (Colorado Concept Coatings, CO, USA) with a surface resistivity of ~ 25.6 ohms (measured in lab), indium-zinc oxide coated glass (IZO) (Colorado Concept Coatings, CO, USA) with a surface resistivity of ~ 15.2 ohms (measured in lab), PEDOT-PSS (Clevios P VP al 4083, Germany) modified ITO (P-ITO) and a heavily doped conductive silicon wafer (n-Si [100] with phosphorus dopants, 14-22 ohm-cm (University Wafer, MA, USA). ITO and IZO are cleaned by sequential sonication in acetone and isopropanol for 5 min in each solvent followed by oxygen plasma treatment for 5 min. The P-ITO is prepared by first filtering PEDOT:PSS through a Pall Acrodisc 0.45 μm syringe filter (CELLTREAT Scientific Products, LLC, MA, USA), then depositing two layers of PEDOT:PSS by spin coating each layer successively at 6000 rpm onto a plasma cleaned ITO surface, and finally annealing the PEDOT:PSS-ITO at 120 $^{\circ}\text{C}$ for 20 min. The last substrate, n-Si [100] wafer, is etched in 5% HF solution for 3 minutes to remove the surface oxide layer and improve conductivity across the surface. All substrates are approximately 2.54 cm x 2.54 cm squares.

2.3. Electro-assisted self-assembly (EASA)

The electrochemical system consists of a 2.54 cm x 2.54 cm planar graphite electrode (anode, counter electrode) and an ITO, IZO, P-ITO or silicon wafer substrate (cathode, working electrode) that is submerged in the precursor sol solution. The two electrodes are held parallel to each other, one inch apart. A Model 362 Scanning Potentiostat (Princeton Applied Research, TN, USA) is used to apply the current needed for aligning CTAB molecules and generating the hydroxyl ions essential for polycondensation of

silica thin films at the substrate surface. The current is set at a constant 0.75 mA/cm^2 substrate and the EASA time is varied between 10 to 20 seconds (as previously optimized)^{26,27}.

2.4. Characterization

After EASA, the resulting structure consisted of CTAB molecules surrounded by silica. The final step to producing mesoporous silica films involved removal of the CTAB to create open pores. This is accomplished by immersing the sample in a 0.01 M HCl ethanol-water solution (50:50 v/v) for 30 minutes under stirring.^{26,27} FTIR characterization confirmed the complete removal of surfactant from the silica film on Si wafer (see Supplementary Information). For metal oxides, the CTAB can also be removed by calcination at $300 \text{ }^\circ\text{C}$ for 30 mins.

The silica film's pore-to-pore distance and pore alignment on the silicon wafer and P-ITO substrates are characterized by Grazing Incidence Small Angle X-ray Scattering (GISAXS) using a Nonius Kappa-CCD diffractometer equipped with an Apex II CCD detector (copper cathode ($\lambda_{\alpha_1} = 0.154184 \text{ nm}$)).

Cross-sectional scanning electron microscope (SEM) images of the silica films to confirm film formation and determine thickness are obtained at a 13° tilt using a JEOL JSM-7000F field emission SEM (JEOL USA, Inc. MA, USA) with an EDAX Genesis energy dispersive X-Ray spectrometer in TSL electron backscatter diffraction mode. Top views showing the size and uniformity of the silica mesopores are obtained with a Phillips CM200 transmission electron microscope (Amsterdam, Netherlands) coupled with a Princeton Gamma-Tech prism energy dispersive X-Ray spectrometer. TEM samples were prepared by either using a razor blade to mechanically scrape the silica

template from the cathode onto the TEM grid or using a liftoff method (described later) that preserves knowledge of the film orientation.

The surface roughness of cleaned substrates is measured with a Digital Instruments Nanoscope III multimode atomic force microscopy (AFM) (CA, USA) using SiN tips with tip curvature less than 10 nm and operating in tapping mode. The surface roughness is also measured by a Tencor P-10 Surface Profiler (CA, USA).

3. Results and Discussion

Reactions pertinent to the preparation of silica films with mesopores oriented perpendicular to the substrate surface are shown in Scheme 1. The first step (Scheme 1A) is the acid catalyzed hydrolysis of TEOS. The pH of the precursor sol and the hydrolysis temperature play important roles in the subsequent formation of the desired mesoporous silica films. The second step is the EASA process which involves the simultaneous electrochemically driven self assembly of cationic surfactants, electro-generation of hydroxide ions (Scheme 1B) and hydroxyl ions catalyzed polycondensation of silica (Scheme 1C) at the cathode/substrate surface.

The effect of precursor sol conditions and substrate surface roughness on the formation of aligned and ordered mesopores are investigated. The resultant silica films are characterized with respect to their thickness, pore size, orientation, and uniformity.

3.1. Optimization of mesoporous silica film formation

3.1.1. Effect of sol pH

The pH of the precursor sol is important for the formation of uniform silica films because there must be sufficient amounts of hydrolyzed TEOS for polycondensation, but without a large excess of H^+ in solution. The optimum pH is determined by maintaining a

constant temperature of 25 °C and varying the solution pH. TEM images of the silica films formed on the P-ITO substrate surface are shown in Fig. 1. At pH = 1.0 and 2.0, silica particles (Fig. 1A) and a multilayer silica film (Fig. 1B) are observed, respectively. At low pH, silica condensation can occur in the bulk solution through an acid catalyzed mechanism³³ and lead to the formation of silica particles. Since the pH is below the isoelectric point of silica, the particles are positively charged³⁴ and are attracted to and deposited on the cathode/substrate. At pH = 3.0, the desired silica films with highly ordered aligned nanopores were obtained (Figs. 1C and 1D). At pH = 4.0 and higher (not shown), no silica film is formed. We speculate that an insufficient amount of hydrolyzed TEOS to create a film is produced at this pH.

3.1.2. Effect of sol temperature

EASA was performed using the optimized precursor sols pH (pH 3). Figure 2 shows TEM images of the top view of silica films formed on a P-ITO substrate. Temperatures of 15 °C and 35 °C (Figs. 2A and 2C) produced silica films with varying pore patterns and domains. The 25 °C precursor sol produced a regular array of hexagonally close packed pores across the entire TEM viewing area (Fig. 2B).

3.1.3. Effect of substrate surface roughness

The relative roughness of ITO, P-ITO, and IZO coated glass and heavily doped silicon wafer are qualitatively evaluated by top view SEM and quantified using AFM. The SEM micrographs in Fig 3 show that ITO possesses the roughest surface and that the PEDOT:PSS coating does indeed planarize the ITO surface. These observations are reflected in the AFM root mean square values (RMS) of 4.98±0.37 nm (ITO), 0.96±0.02 nm (P-ITO), 0.08±0.01 nm (Si wafer), and 0.96±0.03 nm (IZO) over a 500 nm x 500 nm

area. (The IZO image also shows the presence of several raised particle-like features which significantly affect the peak-to-valley values and thus these numbers are not reported here.)

TEM images of silica films formed on each substrate are shown in Fig 4. While mesopores are sometimes observed in silica films prepared on ITO coated glass, the quality is low with considerable pore disorder and mis-orientation. In contrast, silica films on PEDOT: PSS modified ITO and heavily doped silicon wafer have hexagonally packed mesopores that extend laterally over several hundred square nanometers. Surprisingly, the silica film on IZO does not exhibit a well defined array of pores despite its comparable RMS to P-ITO. The AFM image of the IZO substrate surface shows small grain sizes that are not apparent on the P-ITO surface (data not shown). The large tilt angles associated with these small grain sizes and their dense packing may hinder coherent micelle assembly during the EASA process. It is possible that substrate surface roughness and the size and density of surface convolutions play an important role in the successful formation of silica films with uniformly aligned mesopores.

3.2. Structural characterization

The orientation of mesopores in silica thin films formed on P-ITO and heavily doped silicon wafer substrates was characterized using 2D GISAXS. The results in Fig. 5 show scattering spots in the equatorial plane in the 2D GISAXS patterns of mesoporous silica films and are indicative of a high level of mesostructural order in the silica film and a vertical orientation of mesopores over several square centimeters. These spots arise from scattering of the (11) and (10) planes of the pore arrays in the silica thin films on P-ITO and Si wafer substrates. The same peaks are also visible in the one dimensional GISAXS

traces derived from Figs. 5A and 5B and shown in Figs. 5C and 5D. The scattering maximum appears at $q_{\max} = 1.722 \pm 0.009 \text{ nm}^{-1}$ and $q_{\max} = 1.699 \pm 0.009 \text{ nm}^{-1}$ for the mesoporous silica films on P-ITO and Si wafer, respectively. From this, the pore periodicities of the samples are found to be $d = 3.65 \pm 0.02 \text{ nm}$ and $3.67 \pm 0.02 \text{ nm}$ for mesoporous silica films on P-ITO and Si wafer, respectively. Taking into account the hexagonal pore pattern, the pore-to-pore distances were determined to be $4.22 \pm 0.02 \text{ nm}$ and $4.23 \pm 0.02 \text{ nm}$. The difference in mesopores sizes measured for the two substrates is $< 0.5\%$. These GISAXS results confirm that the hexagonal patterns in the TEM images of Figs 1D, 2B, and 4B represent vertical pores and not Moire patterns produced by overlapping stripes from the side view of overlaid hexagonally packed mesopores. The faint rings observed in Figs. 5A and 5B are due to spherical silica particles that form on the surface of the mesoporous silica thin films via silica condensation in the bulk solution²⁹.

The silica films formed on P-ITO and heavily doped silicon wafer substrates were further examined by SEM. Cross sectional SEMs in Figs. 6A and B allowed the various layers in the films to be identified and from this, a growth rate could be obtained. Using optimized pH and temperature and holding the current between electrodes constant at 0.75 mA/cm^2 for 10 - 20 s during EASA growth resulted in the formation of 100 – 200 nm thick films (growth rate of 10 nm/s) on both the P-ITO and heavily doped Si wafer substrates. EDX confirmed that the top layer in both SEM images was silica. TEM images show that the silica films formed on both substrates have well-ordered hexagonally packed mesopores that are $\sim 3 \text{ nm}$ in diameter (Fig. 6C and 6D). This is in good agreement with the GISAXS pore-to-pore distance of $\sim 4.2 \text{ nm}$. Uniform mesopores

are observed when different regions of the 6.5 cm² silica film are examined. Figure 6E shows a TEM image of the silica film with a striped pattern that is ~100 nm in length and ~3 nm in width. These dimensions correspond to the measured thickness of the silica film and the size of the mesopores and thus this image is attributed to a cross section view of the silica film. In combination, the GISAXS measurements and electron micrographs provide evidence that the mesopores in the silica film are oriented perpendicular to the substrates' surface. The TEM images of silica film on P-ITO and silicon wafer in Figs 4 and 6 are from different samples and illustrate the reproducibility of the EASA process. The high resolution images confirm the quality of the close packed mesopores.

3.3 Using PEDOT:PSS to obtain free standing silica thin films

The ability to form mesoporous silica films on substrates coated with conducting organics such as PEDOT:PSS greatly expands the range of substrates and, hence, novel applications. The polymer can be used to planarize rough surfaces and to impart conductivity to insulating substrates. If desired, the PEDOT-PSS coating on P-ITO can be easily eliminated by calcining at 300 °C for 30 mins. This effectively results in a well organized nanoporous silica thin film in contact with a relatively rough metal oxide substrate or an insulating substrate.

Perhaps more importantly, mesoporous film formation on a PEDOT:PSS coated substrate opens up the possibility of film liftoff to yield a free standing nanoporous silica film or for direct transfer to an alternative surface on which it would not normally be possible to synthesize such a film. To demonstrate liftoff, narrow strips of two-sided adhesive tape are attached to the outer periphery of a TEM grid. The grid is then pressed

onto the surface of the mesoporous silica thin film formed on a PEDOT:PSS coated ITO substrate to adhere and liftoff the silica film only. The low magnification TEM image of Fig. 7A shows a large section of the silica film positioned on the TEM copper grid. Pore uniformity is clearly maintained as demonstrated by the higher magnification image shown in Fig. 7B. This film transfer has the additional benefit of allowing examination of the pores from the side of the film that was originally attached to the substrate and further confirmed the nanopores' vertical orientation and the interpretation of TEM results shown in earlier figures as "top view". The silica film can also be detached by submersing the sample in water to disperse the PEDOT:PSS and sonicating for 90 s at 135 W and 42 kHz. The released film floated to the surface and was 'fished out' with a TEM grid. Similar results (see Supplementary information) to those shown in Fig. 7 are obtained. Again, in spite of the unoptimized detachment process, the structural integrity of the resulting free standing nanoporous silica film is maintained.

Conclusions

Silica thin films with ~ 3 nm mesopores that are hexagonally packed and aligned perpendicularly to the surface were rapidly synthesized on P-ITO and heavily doped silicon wafer substrates using an electro-assisted self assembly method. Optimum conditions that led to formation of mesoporous films on these surfaces were identified. TEM and GISAXS confirmed the presence of highly ordered mesopores aligned perpendicular to the substrate surface. The use of a PEDOT:PSS layer opened up the possibility for producing aligned mesopores on a much broader range of surfaces and non-conductive substrates. In addition to being a nontraditional conductive substrate, the PEDOT:PSS coated substrates have the additional feature of providing a facile route for

detaching and transferring the silica film to other substrates and for forming free standing mesoporous silica thin films.

Acknowledgments

This material is based upon work supported by the National Science Foundation sponsored Renewable Energy Material Research Science and Engineering Center (REMRSEC) under DMR-0820518. We gratefully acknowledge the assistance of John Chandler and Gary Zito for electron microscopy, David Grosso for GISAXS, Tom Brenner for AFM measurements, and all REMRSEC members for insightful discussions.

References

- 1 C.T. Kresge, M.E. Leonowicz, W.J. Roth, J.C. Vartuli, and J.S. Beck, *Nature*, 1992, **359**, 710.
- 2 D. Zhao, J. Feng, Q. Huo, N. Melosh, G.H. Fredrickson, B.F. Chmelka, and G.D. Stucky, *Science*, 1998, **279**, 548.
- 3 Y. Sakamoto, I. Diaz, O. Terasaki, D. Zhao, J. Perez-Pariente, J.M. Kim, and G.D. Stucky, *J. Phys. Chem. B*, 2002, **106**, 3118.
- 4 J. Fan, C. Yu, T. Gao, J. Lei, B. Tian, L.Wang, Q. Luo, B. Tu, W. Zhou, and D. Zhao, *Angew. Chem. Int. Ed.*, 2003, **42**, 3146.
- 5 C. Gao, Y. Sakamoto, K. Sakamoto, O. Terasaki, and S. Che, *Angew. Chem. Int. Ed.*, 2006, **45**, 4295.
- 6 F. Kleitz, S. Choi, and R. Ryoo, *Chem. Commun.*, 2003, 2136.
- 7 C. Dickinson, W. Zhou, R.P. Hodgkins, Y. Shi, D. Zhao, and H. He, *Chem. Mater.*, 2006, **18**, 3088.

- 8 K. Jiao, B. Zhang, B. Yue, Y. Ren, S. Liu, S. Yan, C. Dickinson, W. Zhou, and H. He, *Chem. Commun.*, 2005, 5618.
- 9 S.H. Woo, and D. Whang, *J. Korean Phys. Soc.*, 2009, **54**, 152.
- 10 N.R.B. Coleman, M.A. Morris, T.R. Spalding, and J.D. Holmes, *J. Am. Chem. Soc.*, 2001, **123**, 187.
- 11 N.R.B. Coleman, N. O'Sullivan, K.M. Ryan, T.A. Croeley, M.A. Morris, T.R. Spalding, D.C. Steytler, J.D. Holmes, *J. Am. Chem. Soc.*, 2001, **123**, 7010.
- 12 P. Xu, H. Yu, and X. Li, *Anal. Chem.*, 2011, **83**, 3448
- 13 P. Innocenzi, L. Malfatti, *Chem. Soc. Rev.*, 2013, **42**, 4198
- 14 D. Grosso, F. Cagnol, G.J.A.A. Soler-Illia, E.L. Crepaldi, H. Amenitsch, A. Brunet-Bruneau, A. Bourgeois, and C. Sanchez, *Adv. Funct. Mater.*, 2004, **14**, 309.
- 15 H. Yang, N. Coombs., and G.A. Ozin, *J. Mater. Chem.*, 1998, **8**, 1205
- 16 M. Lukaschek, D. A. Grabowski, and C. Schmidt, *Langmuir*, 1995, **11**, 3590;
- 17 K. Amundson, E. Helfand, X. Quan, and S. D. Hudson, *Macromolecules*, 1994, **27**, 6559;
- 18 W. Schnepf, S. Disch, and C. Schmidt, *Liq. Cryst.*, 1993, **14**(3), 843
- 19 A. Firouzi, D.J. Schaefer, S.H. Tolbert, G.D. Stucky, and B.F. Chmelka, *J. Am. Chem. Soc.*, 1997, **119**(40), 9466.
- 20 S.H. Tolbert, A. Firouzi, G.D., Stucky, and B.F. Chmelka, *Science*, 1997, **278**, 264.
- 21 Y. Yamauchi, M. Wawada, T. Noma, H. Ito, S. Furumi, Y. Sakka, and K. Kuroda, *J. Mater. Chem.*, 2005, **15**, 1137.
- 22 E. K. Richman, T. Brezesinski, S. H. Tolbert, *Nature Mater.*, 2008, **2**, 712.

- 23 Z. Teng, G. Zheng, Y. Dou, W. Li, C. Mou, X. Zhang, A. M. Asiri, D. Zhao, *Angew. Chem. Int. Ed.*, 2013, **51**, 2173
- 24 P. Stroeve, N. Ileri, *Trends Biotechnol.*, 2011, **29**(6), 259
- 25 Z. P. Huang, N. Geyer, L. F. Liu, M. Y. Li, P. Zhong, *Nanotechnology*, 2010, **21**, 465301
- 26 A. Walcarius, E. Sibottier, M. Etienne, and J. Ghanbaja, *Nature Mater.*, 2007, **6**, 602.
- 27 A. Goux, M. Etienne, E. Aubert, C. Lecomte, J. Ghanbaja, and A. Walcarius, *Chem. Mater.*, 2009, **21**, 731.
- 28 J. W. Dini, *Electrodeposition: The Materials Science of Coatings and Substrates*, Noyes Publications, Norwich NY, 1993
- 29 S. Sayen, and A. Walcarius, *Electrochem. Commun.*, 2003, **5**, 341.
- 30 G. Kavei, Y. Zare, and M. A. Gheidari, *Scanning*, 2008, **30**(3), 232.
- 31 S. Na, G. Wang, S. Kim, T. Kim, S. Oh, B. Yu, T. Lee, and D. Kim, *J. Mater. Chem.*, 2009, **19**, 9045.
- 32 G. Udupa, B. K. A. Ngoi, *Proceedings of the annual meeting-American Society for Precision Engineering*, 2000, 421.
- 33 C.J. Brinker, and G.W. Scherer, *Sol-Gel Science-The Physics and Chemistry of Sol-Gel Processing*, Academic Press, Boston MA, 1990.
- 34 H. E. Bergna, W.O. Roberts, Eds., *Colloidal Silica: Fundamentals and Applications*, Taylor and Francis Group, Boca Raton FL, 2006, p. 273

Figure Captions

Figure 1. TEM images of silica films formed on P-ITO substrates using precursor sols maintained at 25 °C and different pHs. (A) pH = 1.0, (B) pH = 2.0, (C) and (D) pH = 3.0.

Figure 2. TEM images of silica films formed on P-ITO substrates using pH = 3.0 precursor sols and different temperatures (A) T = 15 °C, (B) T = 25 °C, and (C) T = 35 °C.

Figure 3. SEM (top view) images of (A) ITO, (B) P-ITO, (C) heavily doped silicon wafer and (D) IZO.

Figure 4. TEM images of silica films formed on (A) ITO, (B) P-ITO, (C) heavily doped silicon wafer and (D) IZO at precursor sol TEOS hydrolysis of pH = 3.0 and T = 25 °C.

Figure 5. 2D GISAXS pattern of mesoporous silica thin films on different substrates (A) P-ITO and (B) heavily doped silicon wafer; 1D GISAXS pattern of mesoporous silica thin films on (C) P-ITO and (D) heavily doped silicon wafer. Precursor sol pH = 3.0 and T = 25 °C.

Figure 6. Cross sectional SEM images of silica thin films on different substrates (A) P-ITO and (B) heavily doped silicon wafer; TEM images (top view) of silica templates on (C) P-ITO and (D) heavily doped silicon wafer and (E) cross section of a silica template on P-ITO. Precursor sol pH = 3.0 and T = 25 °C.

Figure 7. TEM of silica film after “liftoff” from P-ITO substrate. (A) low magnification image showing a small square of the TEM grid (dark straight rectangles) with a section of silica film and (B) high magnification image of the mesoporous silica film.

Scheme Titles

Scheme 1. Reactions pertinent to the formation of ordered and perpendicularly aligned mesopores.

(A) Acid-catalyzed hydrolysis of TEOS.

(B) Electro-generation of hydroxyl ions on cathode surface.

(C) Hydroxyl ions catalyzed silica sol condensation on cathode surface.

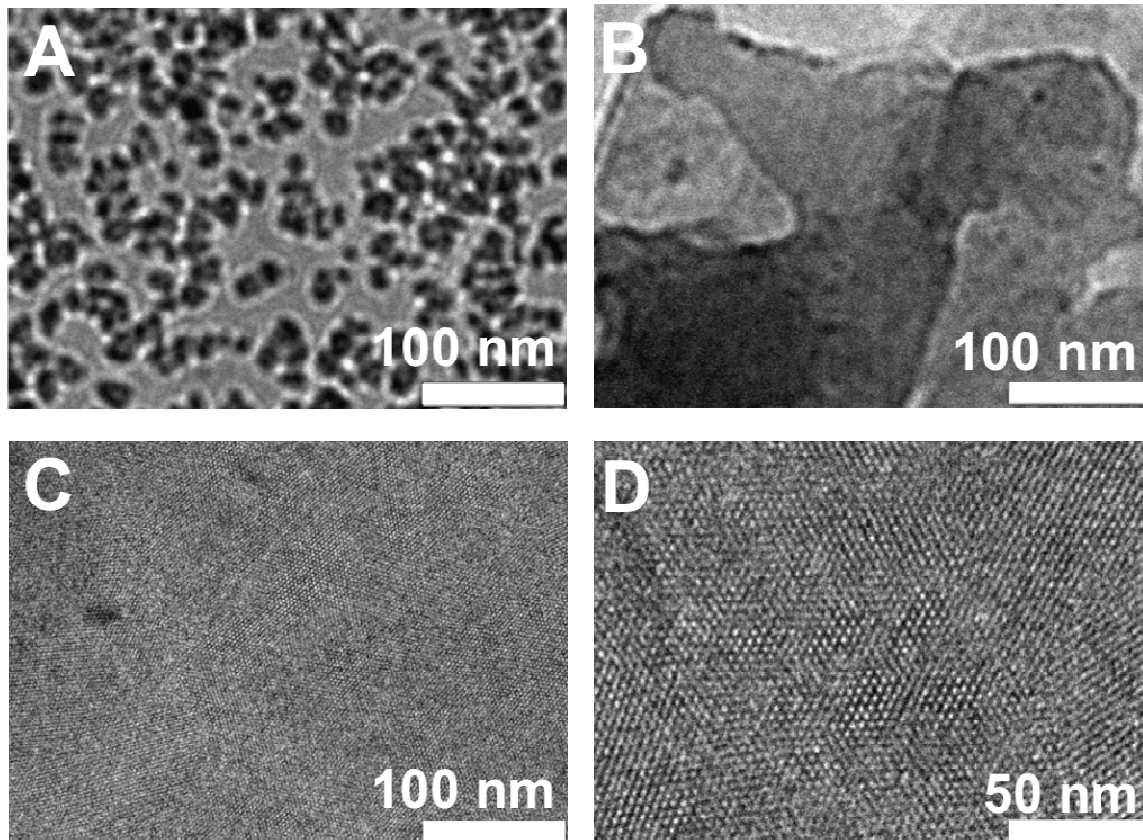


Figure 1.

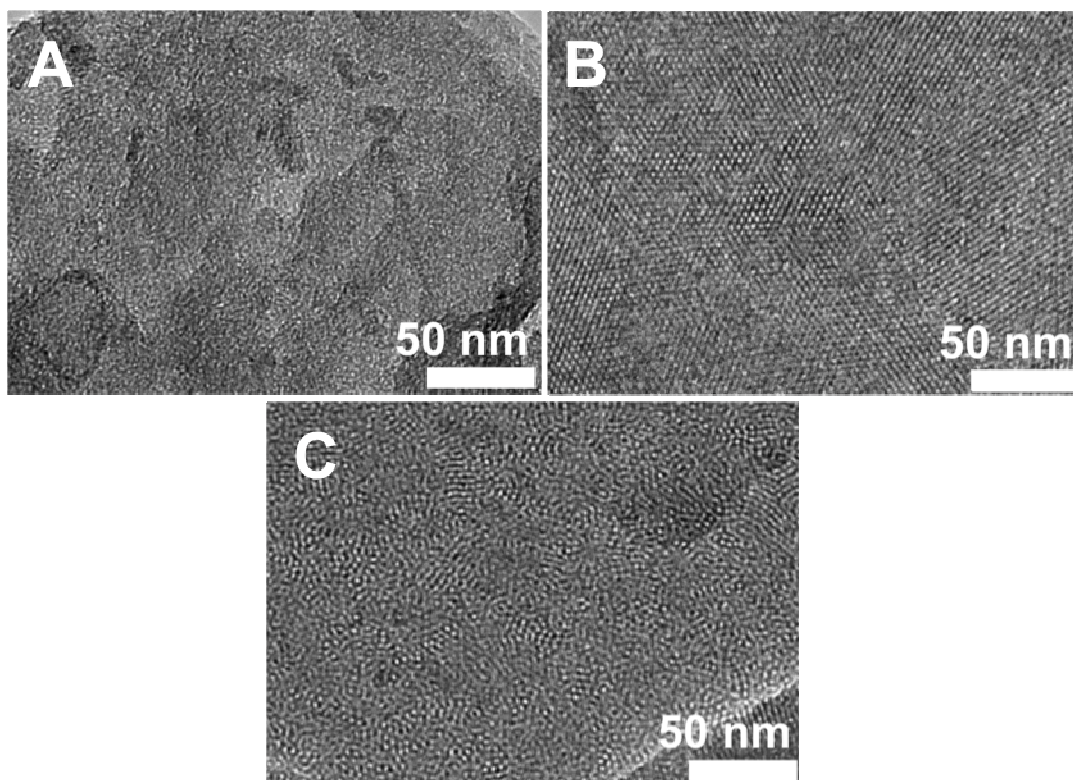


Figure 2.

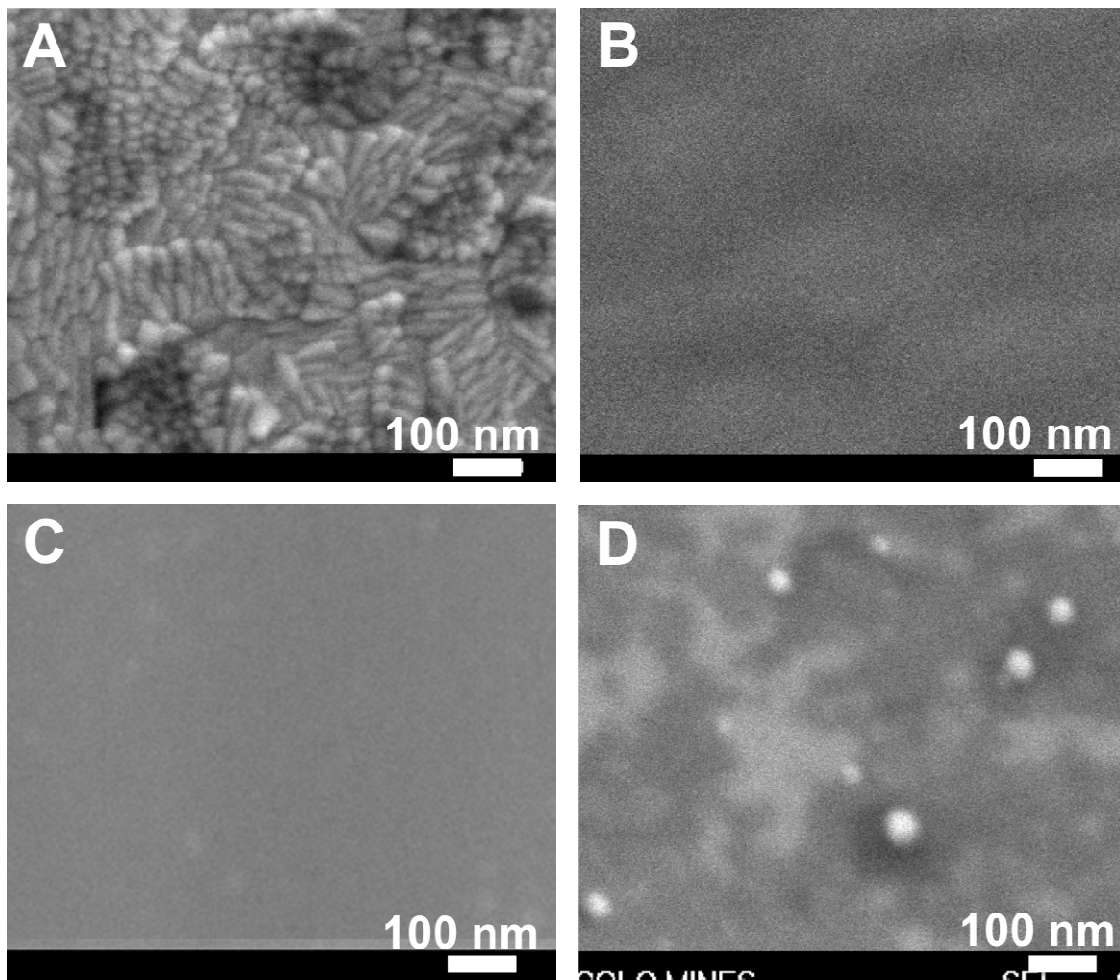


Figure 3.

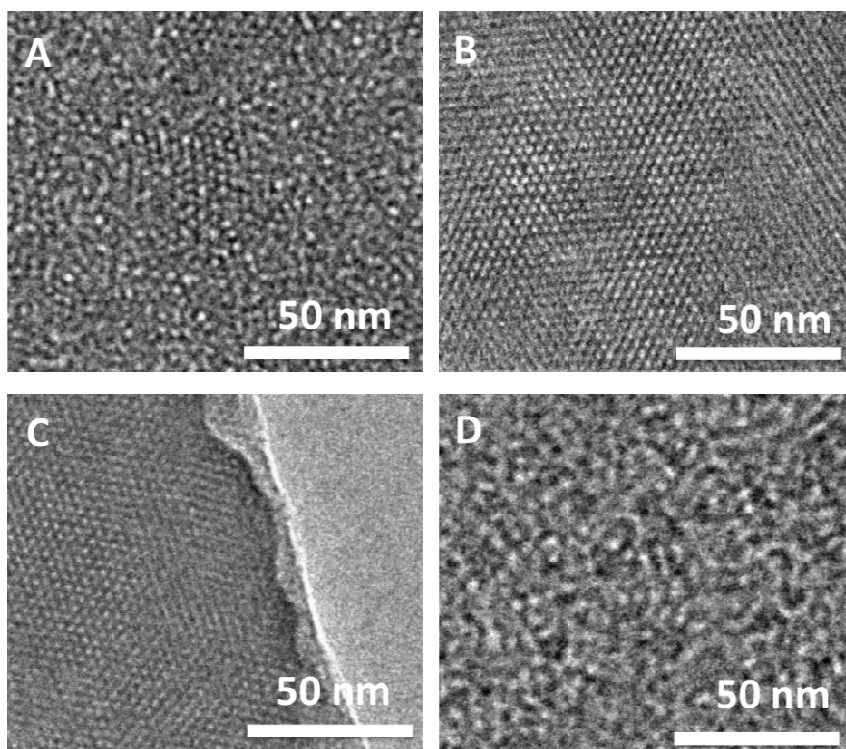


Figure 4.

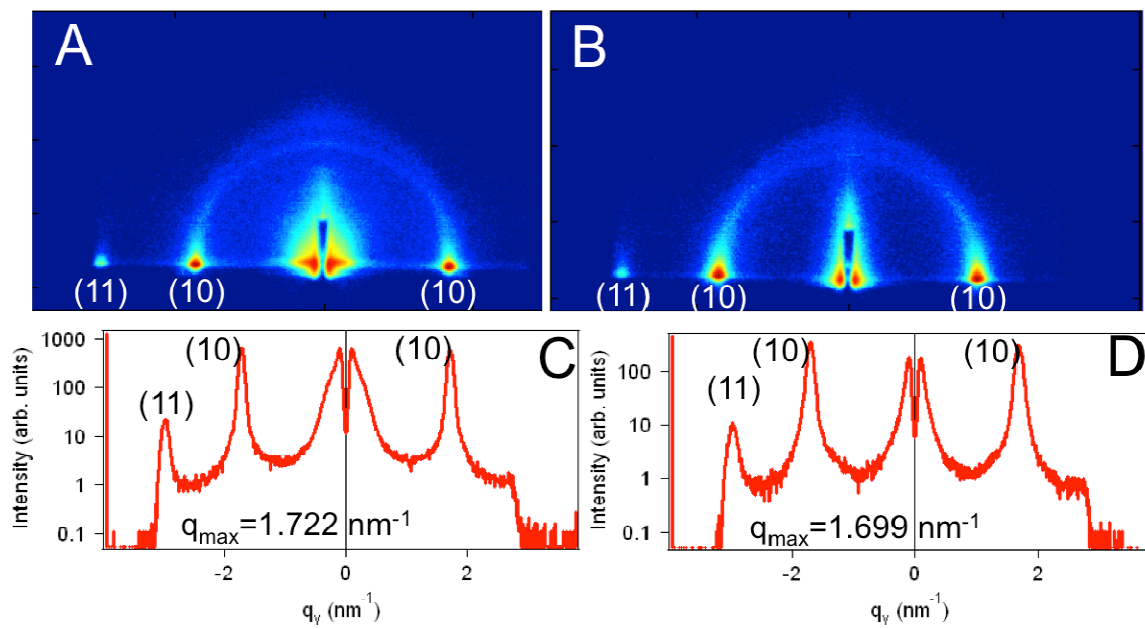


Figure 5.

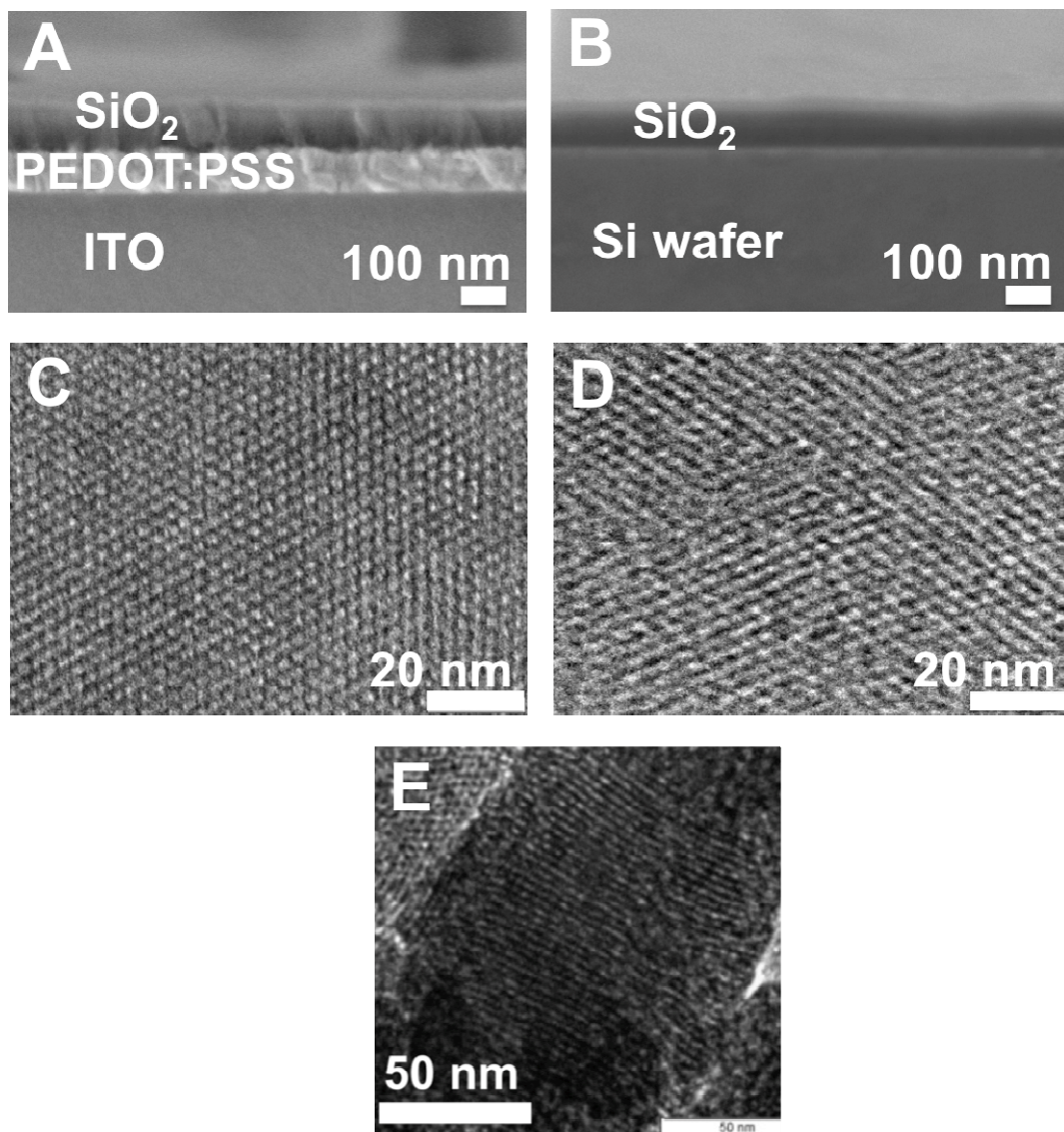


Figure 6.

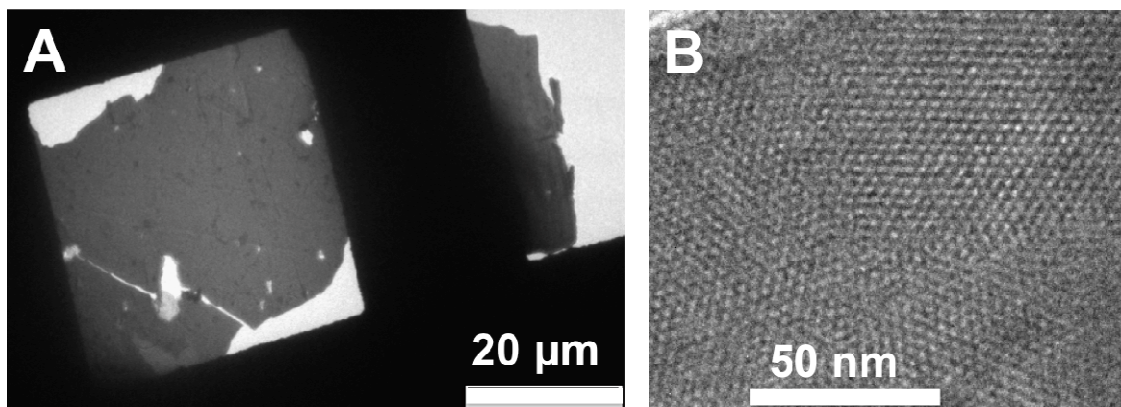
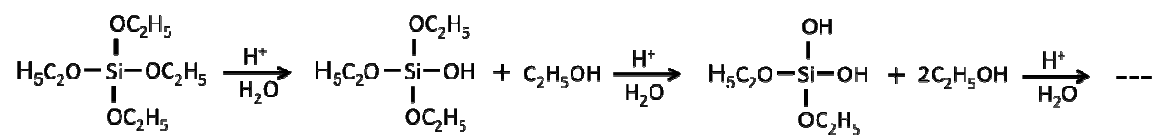


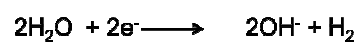
Figure 7.

Scheme 1

A



B



C

